CN^- Secondary Ions Form by Recombination as Demonstrated Using Multi-Isotope Mass Spectrometry of ^{13}C- and ^{15}N-Labeled Polyglycine

G. McMahon, H. Francois Saint-Cyr, and C. Lechene
National Resource for Imaging Mass Spectrometry, Harvard Medical School and Brigham and Women's Hospital, Cambridge, Massachusetts, USA

C. J. Unkefer
National Stable Isotopes Resource, Los Alamos National Laboratory, Los Alamos, New Mexico, USA

We have studied the mechanism of formation CN^- secondary ions under Cs^+ primary ion bombardment. We have synthesized ^{13}C and ^{15}N labeled polyglycine samples with the distance between the two labels and the local atomic environment of the ^{13}C label systematically varied. We have measured four masses in parallel: ^{12}C, ^{13}C, and two of $^{12}C^{14}N^-$, $^{13}C^{14}N$, $^{12}C^{15}N$, and $^{13}C^{15}N$. We have calculated the $^{13}C/^{12}C$ isotope ratio, and the different combinations of the CN isotope ratios ($^{27}CN/^{26}CN$, $^{28}CN/^{27}CN$, and $^{28}CN/^{26}CN$). We have measured a high $^{13}C^{15}N^-$ secondary ion current from the ^{13}C and ^{15}N labeled polyglycines, even when the ^{13}C and ^{15}N labels are separated. By comparing the magnitude of the varied combinations of isotope ratios among the samples with different labeling positions, we conclude the following: CN^- formation is in large fraction due to recombination of C and N; the C=O double bond decreases the extent of CN^- formation compared to the case where carbon is singly bonded to two hydrogen atoms; and double-labeling with ^{13}C and ^{15}N allows us to detect with high sensitivity the molecular ion $^{13}C^{15}N^-$. (J Am Soc Mass Spectrom 2006, 17, 1181–1187) © 2006 American Society for Mass Spectrometry

We are developing the methodology of multi-isotope imaging mass spectrometry (MIMS), which combines a new generation of SIMS instrument, labeling with stable isotopes and quantitative image analysis software [1–4]. We use this methodology to measure molecular turnover in subcellular compartments using stable isotopes, in particular ^{15}N, as tracers. We derive the value of the ^{15}N enrichment from $^{12}C^{15}N/^{12}C^{14}N$ isotope ratio measurements. Although CN^- ion has been used in pioneering biological studies [5], the mechanism of formation of the CN^- molecular ion is not fully understood. There are three possibilities: the recombination of the monatomic sputtered species (e.g., $C + N -> CN^-$), a direct sputtering of CN^- from the sample, or a combination of these two. The recombination mechanism had been proposed in early work [6] based on astute indirect evidence.

To study directly the mechanism of formation of CN^-, we have measured four masses in parallel: $^{12}C^-$, $^{13}C^-$, and two of $^{12}C^{14}N$, $^{13}C^{14}N$, $^{12}C^{15}N$, $^{13}C^{15}N$, and derived the $^{13}C/^{12}C$, $^{27}CN/^{26}CN$, $^{28}CN/^{27}CN$, and $^{28}CN/^{26}CN$ isotope ratios from a series of poly5-glycine samples labeled with ^{13}C and ^{15}N at specific positions in the molecule. We find that CN^- formation is in large fraction due to recombination of C and N, that the high bond strength of the C=O double bond decreases the extent of CN^- formation compared to case where carbon is singly bonded to two hydrogen atoms, and that double-labeling with ^{13}C and ^{15}N allows us to detect with high sensitivity the molecular ion $^{13}C^{15}N^-$.

Experimental

Five types of poly5-glycine (PG2-PG6) labeled with ^{13}C and ^{15}N were synthesized at the National Stable Isotope Resource at Los Alamos National Laboratory. The synthesis of labeled glycine was carried out by a modification of the Gabriel synthesis. Briefly, [^{15}N]-, [1-^{13}C]-, [2-^{13}C]-, [2-^{13}C, ^{15}N]- and [1,2-$^{13}C_2$, ^{15}N]glycine were prepared in separate reactions in which the appropriate isotopomers of ethyl 2-bromoacetate ([1-^{13}C]-, [2-^{13}C]-, or [1,2-$^{13}C_2$]-, or natural abundance) and potassium succinimide ([^{15}N]- or natural abundance) were combined to yield the corresponding labeled N,N-succinoyl glycine ethyl ester [7, 8]. Labeled glycines were de-

Published online June 5, 2006

Address reprint requests to Dr. C. Lechene, NRIMS, Harvard Medical School and Brigham and Women's Hospital, 65 Landsdowne St., Cambridge, MA 02139, USA. E-mail: cpl@harvard.edu

1044-0305/06/$32.00
doi:10.1016/j.jasms.2006.04.031

Received January 20, 2006
Revised April 1, 2006
Accepted April 8, 2006

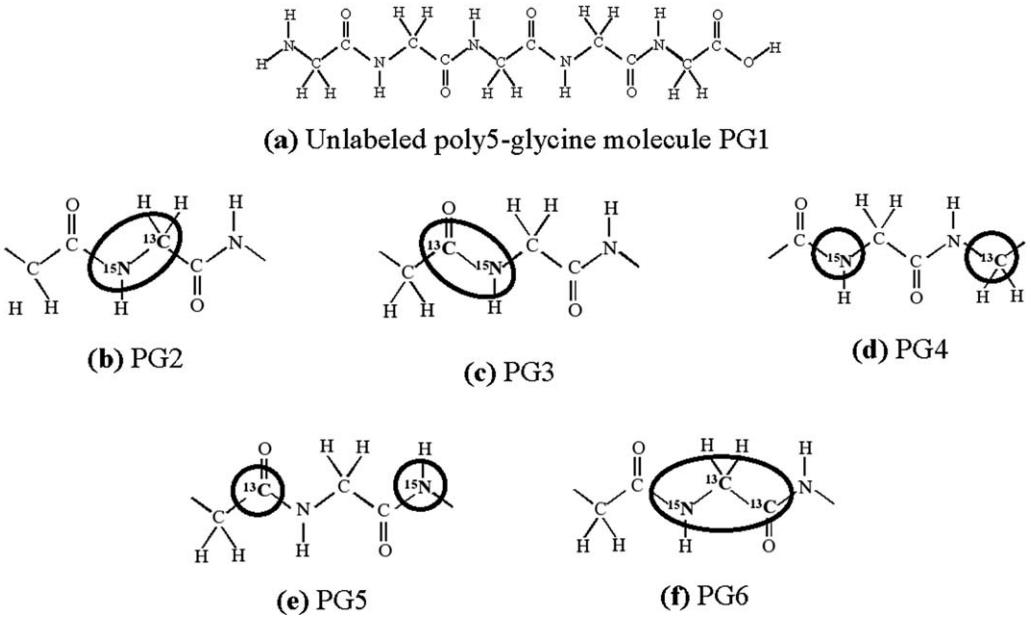

Scheme 1. (**a**) The complete unlabeled polyglycine molecule ($OH[COCH_2NH]_5H$) (PG1). A portion of the unlabeled polyglycine molecule showing relative positions of the ^{13}C and ^{15}N labels for (**b**) sample PG2, (**c**) sample PG3, (**d**) sample PG4, (**e**) sample PG5, and (**f**) sample PG6.

blocked by acid hydrolysis and isolated in their zwitterionic form by ion-exchange chromatography on Dowex AG50X8 (200–400) H^+ (Biorad Laboratories, Hercules, CA). Labeled glycines were prepared as their N-Fmoc derivatives for peptide synthesis by treatment with 9-fluorenylmethyl succinimidyl carbonate (Aldrich Chemical Co., Milwaukee, WI) in the presence of sodium bicarbonate [9]. To determine the position and enrichment of ^{13}C- and ^{15}N-labels, N-Fmoc-[1-^{13}C]glycine, N-Fmoc-[2-^{13}C]glycine, N-Fmoc-[2-^{13}C, ^{15}N]glycine, and N-Fmoc-[1,2-$^{13}C_2$, ^{15}N]glycine samples in [$^2H_6$]DMSO were analyzed by ^1H NMR spectroscopy. N-Fmoc-[1-^{13}C]glycine: {^1H} amide − 6.83 ppm, $^3J_{H\text{-}H}$ = 6.3 Hz, methylene − 3.92 ppm, $^3J_{H\text{-}H}$ = 6.3 Hz, $^3J_{H\text{-}C}$ = 4.2 Hz; N-Fmoc-[2- ^{13}C]glycine:{^1H} amide − 6.83 ppm $^3J_{H\text{-}H}$ = 6.0 Hz, methylene − 3.93 ppm, $^3J_{H\text{-}H}$ = 6.0 Hz, $^1J_{H\text{-}C}$ = 139 Hz; N-Fmoc-[2-^{13}C, ^{15}N]glycine: {^1H} amide − 6.79 ppm, $^3J_{H\text{-}H}$ = 6.0 Hz, $^1J_{H\text{-}N}$ = 94 Hz, $^3J_{H\text{-}C}$ = 3.9 Hz, methylene − 3.93 ppm, $^3J_{H\text{-}H}$ = 6.0 Hz, $^1J_{H\text{-}C}$ = 139 Hz; N-Fmoc-[1,2-$^{13}C_2$, ^{15}N]glycine: {^1H} amide − 6.79 ppm, $^3J_{H\text{-}H}$ = 6.0 Hz, $^1J_{H\text{-}N}$ = 94 Hz, $^3J_{H\text{-}C}$ = 3.9 Hz, methylene − 3.93 ppm, $^3J_{H\text{-}H}$ = 6.0 Hz, $^1J_{H\text{-}C}$ = 139 Hz, and $^3J_{H\text{-}C}$ = 4.2 Hz. These data prove that the labels were incorporated into N-Fmoc glycines without dilution and without scrambling. The peptapeptides Gly-Gly-Gly-Gly-Gly, Gly-Gly-[1,2-$^{13}C_2$, ^{15}N]Gly-Gly-Gly, Gly-Gly-[2-^{13}C, ^{15}N]Gly-Gly-Gly, Gly-Gly-[^{15}N]Gly-[2-^{13}C]Gly-Gly, Gly-[1-^{13}C]Gly-[^{15}N]Gly-Gly-Gly were prepared using a standard Fmoc solid-phase peptide synthesis conditions using a commercial synthesizer (ABI 433A). To increase the peptide yield, unlabeled glycine residues were introduced using a double coupling scheme and a Fmoc-Gly-NovaSyn-TGT resin (Novabiochem, San Diego, CA). To minimize the loss of the label, ^{13}C and/or ^{15}N-glycine residues were introduced with a single coupling step followed by a benzoic acid capping step to terminate nonlabeled peptides. Peptide synthesis was carried out on a 0.25 mmol scale and peptides were released from the resin by treatment with TFA: triisopropylsilane:water (95:2:3). Peptides were purified to >98% by reverse phase HPLC using a Waters SymmetryPrep C_{18} column (7 μM, 19 × 150 mM, Milford, MA) using a 20 ml/m flow rate and a linear gradient of acetonitrile (2-30%) in H_2O (98-70%) containing 0.1% TFA. Using solid-phase peptide synthesis and the capping procedure described above, it is impossible to scramble or dilute the ^{13}C- or ^{15}N-labels during the peptide synthesis. Peptides were characterized by electrospray mass spectrometry using a Thermo Finnigan LTQ in the positive ion mode. The protonated peptides PG1 (304) PG2 (306), PG3 (306), PG4 (306), PG5 (306) and PG6 (307) had the expected nominal masses. Except PG4, all samples with labeled positions were enriched to 99.2% with ^{13}C or and 99% with ^{15}N. The [2-^{13}C]glycine was prepared from [2- ^{13}C]bromo acetic acid that was enriched to only 90% with ^{13}C. So the labeled positions in the peptide PG4 are enriched to 99% with ^{15}N and 90% with ^{13}C.

The relative positions of the ^{15}N and ^{13}C labels for each type of polyglycine are shown in Scheme 1. Sample PG1 is the unlabeled control sample. Samples PG2 and PG3 each contain one ^{13}C and one ^{15}N label substituted for one C and one N atom and bonded to each other. In PG2 the ^{13}C is bonded to two H atoms, while in PG3 ^{13}C is double-bonded to the oxygen atom. In samples PG4 and PG5, the ^{13}C and ^{15}N labels are separated. In PG4 the ^{13}C label is bonded to two H atoms, while in PG5 ^{13}C is double-bonded to the oxygen

Table 1. Secondary ions detected by each of the four electron multipliers (EM1- EM4) in each analysis series

	Detector			
Series	EM 1	EM 2	EM 3	EM 4
A	$^{12}C^-$	$^{13}C^-$	$^{12}C^{14}N^-$	$^{13}C^{14}N^-$
B	$^{12}C^-$	$^{13}C^-$	$^{12}C^{15}N^-$	$^{13}C^{15}N^-$
C	$^{12}C^-$	$^{13}C^-$	$^{12}C^{14}N^-$	$^{12}C^{15}N^-$
D	$^{12}C^-$	$^{13}C^-$	$^{13}C^{14}N^-$	$^{13}C^{15}N^-$
E	$^{12}C^-$	$^{13}C^-$	$^{12}C^{14}N^-$	$^{13}C^{15}N^-$

atom. Sample PG6 contains two ^{13}C labels and one ^{15}N label bonded contiguously, and one of the ^{13}C labels is double-bonded to an oxygen atom.

We dissolved the samples in 1 ml deionized water to concentrations ranging from 7.3×10^{-2} M to 1.3×10^{-1} M. They were distributed in 20 vials of 50 μl-aliquots and kept frozen at −80 °C.

We prepared the samples by depositing microdroplets from capillary glass made from pulled Pasteur pipettes onto the surface of a 5.0 mm by 5.0 mm Si chip (Montco Silicon Technologies Inc., Spring City, PA) under a stereomicroscope (OpMi-1, Carl Zeiss, West Germany). We cut the Si chips to size at Microsystems Technology Laboratories, MIT, Cambridge, MA (see http://www.nrims.harvard.edu/protocols.php). We dried the specimens in air and kept them in a vacuum oven (Fisher Scientific Isotemp Vacuum Oven 280A, Pittsburgh, PA) at 50 °C before loading into the instrument for analysis.

We analyzed the samples with the prototype of the NanoSIMS50 (Cameca Inc., Courbevoie, France). We used a beam of Cs^+ primary ions with a net impact energy on the sample of 16 keV to sputter the material and produce secondary ions. The primary ion beam current was 5.85 pA. We recorded mass spectra from each detector and set the EM deflection voltages to measure the secondary ion count rate [1, 10]. We measured in parallel four ion masses sputtered from the same sample volume and detected simultaneously by four electron multipliers (EM1–EM4). The electron multipliers efficiencies were balanced [1]. We performed five series of analyses on each polyglycine sample, measuring different combinations of $^{26}CN^-$, $^{27}CN^-$, or $^{28}CN^-$ on EM3 and EM4 and $^{12}C^-$ and $^{13}C^-$ on EM1 and EM2 in all series (Table 1). We have analyzed each series at least twice. We used a counting time of 1 s/data point and corrected for the dead time of the electron multiplier. We acquired one hundred data points at each mass per analysis, and we calculated the isotope ratios in blocks of ten by averaging the ten isotope ratio values within each block. This yielded 10 values of the isotope ratio per analysis set. The analyses were obtained from different areas of the drop, separated by ~30–40 μm. We used Prophet statistical software (NIH, NCRR) for statistical analysis providing values for the mean, the standard deviation (s.d.) and the standard error of the mean (s.e.m.) of the isotope ratios. We removed the few data outliers using the Dixon test. In all cases the isotope ratio value for sample PG4 has been adjusted to account for the 90% labeling.

From the composition of the samples (Scheme 1), the isotope ratio values we expected for the $^{13}C/^{12}C$ and $^{15}N/^{14}N$ isotope ratios were for PG1: the natural abundance values 1.12% and 0.367%, respectively, for PG2–PG5: 12.3% and 25.5% respectively, and for PG6: 26.4% and 25.5%, respectively.

Results and Discussion

In any of the analysis series, the values of the $^{13}C/^{12}C$ and the $^{27}CN/^{26}CN$ isotope ratios were within a few percent of the natural abundance for the control sample PG1, and were all increased in the labeled samples (summarized in Table 2). The magnitude of these increases will be described below.

$^{13}C/^{12}C$ Ratios—All Series

The $^{13}C/^{12}C$ isotope ratio values for all polyglycine samples are summarized in Figure 1. The mean value of the $^{13}C/^{12}C$ ratio (1.05%, standard deviation s.d. = 0.03, N = 134) for the reference sample PG1 is very close to the predicted value. The isotope ratio values for the labeled samples are all elevated. Sample PG2 (13.7%, s.d. = 0.6%, N = 231), PG4 (13.2%, s.d. = 0.9%, N = 160), and PG6 (23.1%, s.d. = 0.9%, N = 212) are very close to the predicted isotope ratios. Samples PG3 (7.11%, s.d. = 0.30%, N = 281) and PG5 (8.41%, s.d. = 0.42%, N = 159) are 42 and 32%, respectively, lower than predicted. The isotope ratios for PG2 and PG4 are very close. We find a larger difference in the isotope ratios between PG3 and PG5.

$^{13}C^{14}N/^{12}C^{14}N$ Ratios—Series A

The $^{13}C^{14}N/^{12}C^{14}N$ isotope ratio values, which is another way to measure the $^{13}C/^{12}C$ ratio, are summarized in Figure 2. The control sample PG1 (1.16%, s.d. = 0.02%, N = 20) is very close to the natural $^{13}C/^{12}C$ ratio. The isotope ratios for the labeled samples are all elevated. Samples PG2 (11.0%, s.d. = 2.0%, N = 30), PG4 (14.0%, s.d. = 0.7%, N = 30), and PG6 (21.4%, s.d. = 0.3%, N = 30) are very close to the predicted values. Samples PG3 (6.30%, s.d. = 0.50%, N = 49) and PG5 (8.79%, s.d. = 0.15%, N = 27) are 49 and 29%, respectively, lower than predicted. The isotope ratio for sample PG4 is higher than for PG2, and the isotope ratio for sample PG5 is higher compared to sample PG3.

$^{13}C^{15}N/^{12}C^{15}N$ Ratios—Series B

The $^{13}C^{15}N/^{12}C^{15}N$ isotope ratio values, which is another way to measure the $^{13}C/^{12}C$ ratio, are shown in Figure 3. The control sample PG1 (1.19%, s.d. = 0.26%, N = 30) is very close to the natural $^{13}C/^{12}C$ isotope ratio. The isotope ratio values for the labeled samples

Table 2. Summary of results from all analysis series. The standard deviation is given in parentheses

Sample	All series $^{13}C/^{12}C$	Series A $^{13}C^{14}N/^{12}C^{14}N$	Series B $^{13}C^{15}N/^{12}C^{15}N$	Series C $^{12}C^{15}N/^{12}C^{14}N$	Series D $^{13}C^{15}N/^{13}C^{14}N$	Series E $^{13}C^{15}N/^{12}C^{14}N$
PG1 (control)	1.05% (0.03)	1.16% (0.02)	1.19% (0.26)	0.377% (0.007)	0.387% (0.048)	0.00452% (0.00010)
PG2 (^{13}C and ^{15}N adjacent)	13.7% (0.6)	11.0% (2.0)	26.1% (1.7)	26.5% (1.0)	45.6% (8.7)	5.18% (0.25)
PG3 (^{13}C and ^{15}N adjacent; ^{13}C bonded to O)	7.11% (0.30)	6.30% (0.50)	18.6% (2.3)	22.9% (1.5)	65.1% (8.6)	2.66% (0.14)
PG4 (^{13}C and ^{15}N separated)	13.2% (0.9)	14.0% (0.7)	12.1% (0.3)	28.2% (0.5)	23.5% (2.1)	3.12% (0.13)
PG5 (^{13}C and ^{15}N separated; ^{13}C bonded to O)	8.41% (0.42)	8.79% (0.15)	8.18% (0.36)	25.8% (0.4)	23.2% (0.5)	1.80% (0.14)
PG6 (two ^{13}C labels; ^{13}C and ^{15}N adjacent; ^{13}C bonded to O)	23.1% (0.9)	21.4% (0.3)	29.9% (4.6)	22.9% (0.8)	31.0% (3.0)	6.30% (0.19)

are all elevated. Only the isotope ratio for PG4 (12.1%, s.d. = 0.3%, N = 40) is close to that expected. The isotope ratio for PG2 (26.1%, s.d. = 1.7%, N = 48) is almost double that and the isotope ratio for PG3 (18.6%, s.d. = 2.3%, N = 55) is about 1.5 times greater than expected. Sample PG5 (8.18%, s.d. = 0.36%, N = 40) is 33% lower than predicted. The ratio for PG6 (29.9%, s.d. = 4.6%, N = 50) is slightly higher than the expected isotope ratio.

$^{12}C^{15}N/^{12}C^{14}N$ Ratios—Series C

The $^{12}C^{15}N/^{12}C^{14}N$ ratios represent the $^{15}N/^{14}N$ ratio and are shown in Figure 4. The ratio for the control sample PG1 (0.377%, s.d. = 0.007%, N = 19) is very close to the natural isotope ratio. The isotope ratios for the labeled samples are all elevated. The isotope ratios for PG2 (26.5%, s.d. = 1.0%, N = 40), PG3 (22.9%, s.d. = 1.5%, N = 40), PG4 (28.2%, s.d. = 0.5%, N = 29), PG5 (25.8%, s.d. = 0.4%, N = 40), and PG6 (22.9%, s.d. = 0.8%, N = 30) are all within 10% of the predicted value.

$^{13}C^{15}N/^{13}C^{14}N$ Ratios —Series D

The $^{13}C^{15}N/^{13}C^{14}N$ ratios, which is another way to measure the $^{15}N/^{14}N$ isotope ratio, are shown in Figure 5. The value of the isotope ratio for the control sample PG1 (0.387%, s.d. = 0.048%, N = 39) is very close to the natural abundance ratio. The isotope ratio values for the labeled samples are all elevated. Samples PG4 (23.5%, s.d. = 2.1%, N = 40) and PG5 (23.2%, s.d. = 0.5%, N = 40) are close to the expected isotope ratio value and to each other. Samples PG2 (45.6%, s.d. = 8.7%, N = 100) and PG3 (65.1%, s.d. = 8.6%, N = 100) are much higher than expected. PG6 is about 20% higher than expected.

$^{13}C^{15}N/^{12}C^{14}N$ Ratios —Series E

The $^{13}C^{15}N/^{12}C^{14}N$ isotope ratio values are shown in Figure 6. The expected value for the $^{13}C^{15}N/^{12}C^{14}N$ ratio based on the natural abundance is 0.00413%, negligible for biological applications. The measured experimental value from PG1 of 0.00452% (s.d. = 0.00010%, N = 30) is within 10% of the expected ratio. The isotope ratios for the labeled samples are all ele-

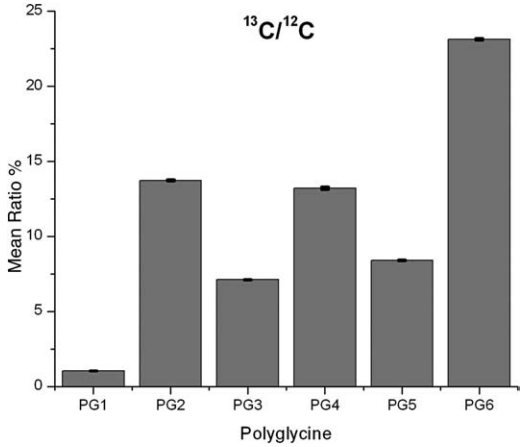

Figure 1. Effect of the environment of the ^{13}C and ^{15}N labels on the $^{13}C/^{12}C$ isotope ratio for all six polyglycine samples. Error bars: standard error of the mean.

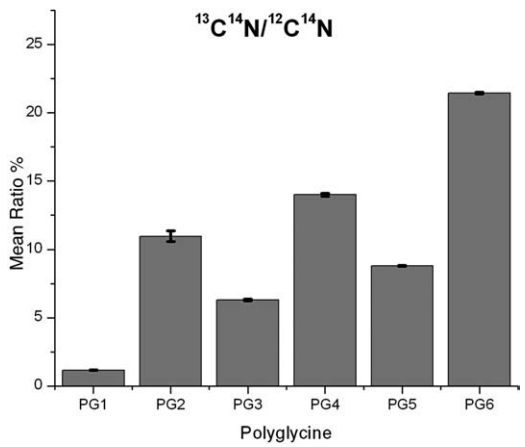

Figure 2. Effect of the environment of the ^{13}C and ^{15}N labels on the $^{13}C^{14}N/^{12}C^{14}N$ isotope ratio for all six polyglycine samples. Error bars: standard error of the mean.

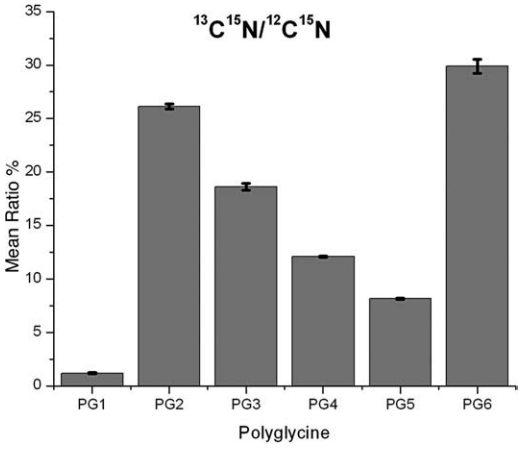

Figure 3. Effect of the environment of the ^{13}C and ^{15}N labels on the $^{13}C^{15}N/^{12}C^{15}N$ isotope ratio for all six polyglycine samples. Error bars: standard error of the mean.

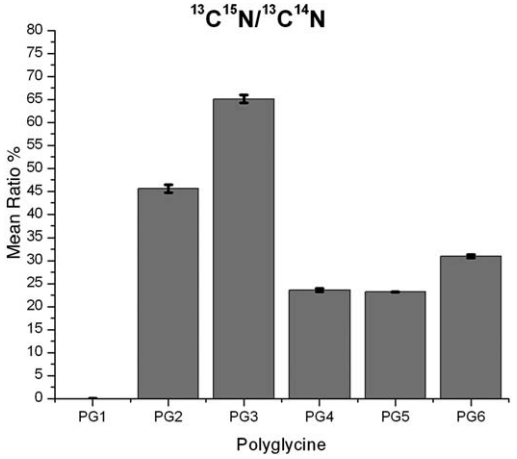

Figure 5. Effect of the environment of the ^{13}C and ^{15}N labels on the $^{13}C^{15}N/^{13}C^{14}N$ isotope ratio for all six polyglycine samples. Errors bars: standard error of the mean.

vated relative to the expected value of 0.00413%. The isotope ratio for sample PG6 (6.30% s.d. = 0.19%, N = 42) is highest, followed by PG2 (5.18%, s.d. = 0.25%, N = 27), PG4 (3.12% s.d. = 0.13%, N = 30), PG3 (2.66%, s.d. = 0.14%, N = 28), and finally PG5 (1.80%, s.d. = 0.14%, N = 30).

Discussion

The results lead to three conclusions: (1) CN^- formation is in large part occurring by a recombination of monatomic C and N, (2) there is a higher probability of CN^- formation when the C and N are bonded to one another, and (3) less monatomic C is sputtered when it is double-bonded to oxygen instead of singly bonded to two hydrogen atoms.

We discuss these conclusions in more detail in the following sections.

CN^- Formation by Recombination

The results demonstrate that CN^- ions are forming in large part by a recombination of monatomic C and N. This clearly springs from the data presented for the $^{13}C^{15}N/^{12}C^{14}N$ (Figure 6), $^{13}C^{15}N/^{12}C^{15}N$ (Figure 3), and $^{13}C^{15}N/^{13}C^{14}N$ (Figure 5) isotope ratios. All of the isotope ratios for the labeled samples in these three sets of data are elevated, indicating a high yield of the $^{13}C^{15}N^-$ ion. Because the ^{13}C and ^{15}N labels are separated in samples PG4 and PG5, the only way the $^{13}C^{15}N^-$ ion could have formed in abundance is by a recombination of monatomic ^{13}C and ^{15}N. The CN^- formation by recombination of monatomic C and N is also observed in the $^{13}C^{14}N/^{12}C^{14}N$ ratios (Figure 2). The isotope ratio values are all elevated. Yet in samples PG2 and PG3 there are no ^{13}C and ^{14}N atoms bonded together. The high yield of $^{13}C^{14}N^-$ in this pair of samples must be a result of the recombination of monatomic ^{13}C and ^{14}N. Our results provide direct

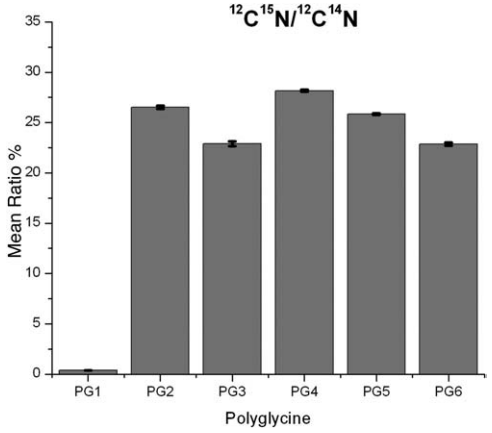

Figure 4. Effect of the environment of the ^{13}C and ^{15}N labels on the $^{12}C^{15}N/^{12}C^{14}N$ isotope ratio for all six polyglycine samples. Error bars: standard error of the mean.

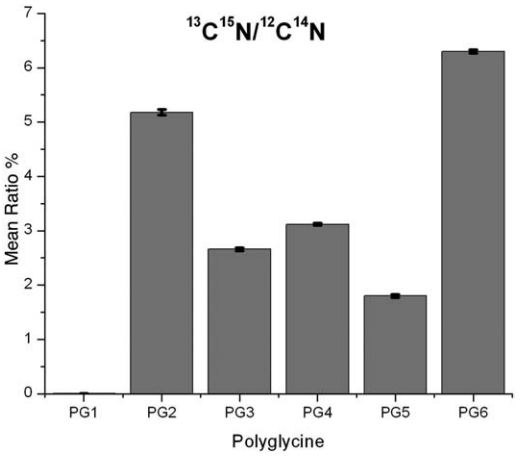

Figure 6. Effect of the environment of the ^{13}C and ^{15}N labels on the $^{13}C^{15}N/^{12}C^{14}N$ isotope ratio for all six polyglycine samples. Error bars: standard error of the mean.

proof of CN formation by recombination of monatomic C and N. Such a mechanism had been proposed by Hindie et al. [6] based on astute indirect evidence.

Although all ^{13}C and ^{15}N labeled samples had a higher $^{13}C^{15}N^-$ ion yield, it was significantly lower when the ^{13}C and ^{15}N labels were separated (PG4 and PG5) than when they were bonded together (PG2 and PG3).

Although CN^- secondary ion currents are higher when ^{13}C and ^{15}N are bonded together, we cannot prove that direct sputtering is occurring by ruling out that adjacent C and N atoms are sputtered in monatomic form and recombine to form the cyanide ion. We are also unable to determine whether the CN^- ion forms by the recombination of C^- and N, or by ionization of molecular CN.

A higher probability of recombination when the ^{13}C and ^{15}N labels are bonded together may explain why the $^{13}C^{15}N/^{13}C^{14}N$ ratios for PG2 and PG3 (45.6% and 65.1%, respectively) are much higher than that expected (25.5%). If adjacent ^{13}C and ^{15}N atoms are more likely to recombine to form the $^{13}C^{15}N^-$ ion, much of the ^{13}C label will be consumed. Fewer ^{13}C atoms will be available to recombine with ^{14}N to form the $^{13}C^{14}N^-$ ion. The net effect is an increase in the numerator $^{13}C^{15}N^-$ counts and a decrease in the denominator $^{13}C^{14}N^-$ counts, resulting in high isotope ratios. The converse is true for samples PG4 and PG5.

Effect of the Carbon-Oxygen Double Bond

We found a decrease in the $^{13}C/^{12}C$ (Figure 1), $^{13}C^{14}N/^{12}C^{14}N$ (Figure 2), $^{13}C^{15}N/^{12}C^{15}N$ (Figure 3), and the $^{13}C^{15}N/^{12}C^{14}N$ (Figure 6) isotope ratios when the ^{13}C label is double-bonded to oxygen. We observe this by comparing samples where all parameters are the same except the bonding configuration of the ^{13}C label (PG2 with PG3 and PG4 with PG5). We found that in each case, the isotope ratio value for PG2 was significantly higher than that of PG3, and that the isotope ratio value for PG4 was significantly higher than that of PG5. Since there is an abundance of ^{12}C in all samples, these results imply that fewer monatomic ^{13}C atoms are sputtered and ionized when they are double-bonded to the oxygen atom. This may be due to the greater bond energy for the C=O double bond (172 kcal/mol) than for the C—N, C—H, and C—C bonds (69.7, 93.8, and 83.1 kcal/mol, respectively [11]. When fewer ^{13}C atoms are sputtered, the result is a lower value for the $^{13}C/^{12}C$ isotope ratio, and also in lower values for the $^{13}C^{14}N/^{12}C^{14}N$, $^{13}C^{15}N/^{12}C^{15}N$, and the $^{13}C^{15}N/^{12}C^{14}N$ isotope ratios through a lowering of the probability of $^{13}CN^-$ ion formation by recombination.

We have shown that the isotope ratio results presented can be explained by the increased probability of CN^- ion formation by recombination of monatomic C and N when they are bonded to each other and when the C atom is singly bonded to two hydrogen atoms as opposed to being double-bonded to the oxygen atom. We cannot, however, explain the difference in the $^{13}C/^{12}C$ ratio for samples PG3 (7.11%, s.d. = 0.30%, N = 281) and PG5 (8.41%, s.d. = 0.42%, N = 159). The isotope ratio values should be equivalent. The only explanation for the discrepancy is an inadvertent dilution of sample PG3 by an extraneous carbonaceous material.

Implications for Tracer Isotope Studies

The data presented in Figure 6 for the $^{13}C^{15}N/^{12}C^{14}N$ ratios has significant practical implications. The sample PG1 has essentially no background. Use of the $^{13}C^{15}N/^{12}C^{14}N$ ratio from a control sample will provide a much lower background ratio (0.00413%) compared to $^{12}C^{15}N/^{12}C^{14}N$ (0.368%). The net effect gained by double-labeling and using the $^{13}C^{15}N$ $^{/12}C^{14}N$ isotope ratio for protein turnover studies as opposed to a conventional single label experiment using the $^{12}C^{15}N/^{12}C^{14}N$ isotope ratio is a factor of 16 increase in the peak to background ratio. The design and use of double-labeled samples should allow measurement of C and N isotope ratios in subcellular domains with an increase in sensitivity.

The conclusions of this work apply to pure samples with tailored labeling and at high isotope label concentration. They do not impact biological experiments using isotope tracers. In biological experiments, the isotope used as a tracer is at low concentration and is metabolized and incorporated at a variety of positions in the metabolite molecules [12]. Thus, the effects observed in this work are likely to be negligible for interpreting changes in isotope ratios in conditions of biological experiment.

Conclusions

We provide direct evidence that the mechanism of formation of the CN^- ion is in large fraction a recombination of monatomic C and N. We show that there is an increased probability of CN^- formation when the C and N are bonded together in the polyglycine molecule.

We demonstrate a strong effect of the bonding configuration of the ^{13}C atom. When it is double-bonded to the O atom rather than singly bonded to two hydrogen atoms, the $^{13}C/^{12}C$, $^{13}C^{14}N/^{12}C^{14}N$, $^{13}C^{15}N/^{12}C^{15}N$, and $^{13}C^{15}N/^{12}C^{14}N$ isotope ratios decrease by 30–50%. We interpret this as being due to a reduction in the sputter yield of ^{13}C due to the greater strength of the double-bond.

We also observe an increase in the peak to background ratios by a factor of 16 when comparing the $^{13}C^{15}N/^{12}C^{14}N$ and $^{12}C^{15}N/^{12}C^{14}N$ isotope ratios. Thus, the design and use of double-labeled samples may allow one to measure C and N isotope ratios in subcellular domains with an increase in sensitivity.

Acknowledgments

This work was supported in part by the NIH under grant 5P41EB001974-05 (CL), grant 5RO1DC004179-03 (CL), and grant P41 5P41EB002166 (CJU).

References

1. Lechene, C.; Hillion, F.; Cotanche, D. A.; McMahon, G.; Benson, D.; Kleinfeld, A. M.; Kampf, J. P.; Distel, D.; Luyten Y.; Bonventre, J.; Hentschel, D.; Park K. M.; Ito, S.; Schwartz, M.; Benichou, G.; Slodzian, G. High resolution quantitative imaging of mammalian and bacterial cells using stable isotope mass spectrometry. *J. Biol.* **2006**, in press.
2. McMahon, G.; Glassner, B. J.; Lechene, C. P. Quantitative imaging of cells with multi-isotope imaging mass spectrometry (MIMS)—Nanoautography with stable isotope tracers. *Proceedings of the 15th International Conference on Secondary Ion Mass Spectrometry—SIMS XV*, *Appl. Surf. Sci.* **2005**, in press.
3. Kleinfeld, A. M.; Kampf, J. P.; Lechene, C. Transport of ^{13}C-oleate in adipocytes measured using multi-isotope imaging mass spectrometry. *J. Am. Soc. Mass Spectrom.* **2004,** *15,* 1572–1580.
4. Hallegot, P.; Peteranderl, R.; Lechene, C. In-situ imaging mass spectrometry analysis of melanin granules in the human hair shaft. *J. Invest. Dermatol.* **2004,** *122,* 381–386.
5. Hindie, E.; Coulomb, B.; Beaupain, R.; Galle, P. Mapping the cellular distribution of labeled molecules by SIMS microscopy. *Biol. Cell* **1992,** *74,* 81–88.
6. Hindie, H.; Blaise, G.; Galle, P. Origin of the CN^- secondary ions emitted from biological tissue under 10 keV Cs^+ bombardment. In Proceedings of the Secondary Ion Mass Spectrometry SIMS XII International Conference; Wiley: Chichester, UK, 1990; p 335.
7. Roberts, J. L.; Poulter, C. D.; 2′3′5′-Tri-O-benzoyl [4- ^{13}C] uridine. An efficient, regiospecific synthesis of the pyrimidine ring. *J. Org. Chem.* **1978,** *43,* 1547–1550.
8. Ott, D. G. Synthesis with stable isotopes of carbon, nitrogen and oxygen; John Wiley and Sons: New York, 1981; pp 33–41.
9. Paquet, A. Introduction of 9-fluorenylmethyloxycarbonyl, trichloroethoxycarbonyl, and benzyloxycarbonyl amine protecting groups into O-unprotected hydroxyamino acids using succinimidyl carbonates. *Can. J. Chem.* **1982,** *60,* 976–980.
10. Peteranderl, R.; Lechene, C. Measurement of carbon and nitrogen stable isotope ratios in cultured cells. *J. Am. Soc. Mass Spectrom.* **2004,** *15,* 478–485.
11. Pauling, L. *College Chemistry*, 3rd ed.; W. H. Freeman and Company: San Francisco and London, 1989; p 316.
12. Schoenheimer, R. The dynamic state of body constituents, *The Edward K. Dunham lectures for the promotion of the medical sciences 1941*; Harvard University Press: Cambridge, 1942; p 1.